Electrical Bias Dependent Photochemical Functionalization of Diamond Surfaces

Beth M. Nichols,[†] Kevin M. Metz,[†] Kiu-Yuen Tse,[†] James E. Butler,[‡] John N. Russell, Jr.,[‡] and Robert J. Hamers*[,†]

Department of Chemistry, University of Wisconsin−Madison, 1101 University Avenue, Madison, Wisconsin 53706, and Surface Chemistry Branch, Code 6170, Naval Research Laboratory, 4555 Overlook Avenue, SW, Washington, D.C. 20375

Received: April 20, 2006; In Final Form: June 17, 2006

Diamond is an excellent substrate for many sensing and electronic applications because of its outstanding stability in biological and aqueous environments. When the diamond surface is H-terminated, it can be covalently modified with organic alkenes using wet photochemical methods that are surface-mediated and initiated by the ejection of electrons from the diamond. To develop a better understanding of the photochemical reaction mechanism, we examine the effect of applying an electrical bias to the diamond samples during the photochemical reaction. Applying a 1 V potential between two diamond electrodes significantly increases the rate of functionalization of the negative electrode. Cyclic voltammetry and electrochemical impedance measurements show that the 1 V potential induces strong downward band-bending within the diamond film of the negative electrode. At higher voltages a Faradaic current is observed, with no further acceleration of the functionalization rate. We attribute the bias-dependent changes in rate to a field effect, in which the applied potential induces a strong downward band-bending on the negative electrode and facilitates the ejection of electrons into the adjacent fluid of reactant organic alkenes. We also demonstrate the ability to directly photopattern the surface with reactant molecules on length scales of $<25\ \mu$m, the smallest we have measured, using simple photomasking techniques.

Introduction

Diamond is an attractive substrate for a wide variety of applications because of its excellent properties such as high thermal, mechanical, and chemical stability, controllable electrical properties, and optical transparency.[1,2] In many cases, the ability to take advantage of these desirable properties also requires controlling the chemistry of the interfaces between diamond and other materials. One approach to this problem is to functionalize the surface of diamond with molecular or biomolecular layers that can provide specific chemical and/or physical properties. For example, recent studies have demonstrated that functionalized diamond surfaces can be used for applications such as chemical and/or biological sensing.[3−6]

While the excellent physical properties of diamond are well understood, the functionalization of this material with molecular and/or biomolecular species has received much less attention. The high stability of diamond makes it a difficult material to functionalize. Previous approaches to functionalizing diamond surfaces with molecular species have included electrochemical,[7] thermal,[8−11] radical,[12,13] and photochemical[14−16] activation methods. We previously reported molecules bearing an alkene (C═C) group will link to the surface of hydrogen-terminated diamond when illuminated with ultraviolet light at 254 nm, forming a well-defined monolayer film.[16,17] These monolayers are chemically robust and can be used as a starting point for linking biomolecules such as DNA[18] and proteins[3] to the surface and/or conferring properties such as resistance to protein binding.[19,20] While this functionalization procedure is clearly very effective, the ability to functionalize diamond with alkenes using 254 nm light is surprising because diamond and most organic alkenes are essentially transparent at this wavelength. A more detailed study[17] showed that there is no significant difference in reactivity between single-crystal and polycrystalline films and that in both cases the functionalization reaction occurs under conditions where photoelectrons can be ejected from diamond into the organic alkene. On the basis of these and other observations, we proposed that the reaction was initiated by the UV photoemission of electrons and subsequent creation of radical anions in the reactant fluid.

While some aspects of this reaction are understood, many questions remain about the photoelectron ejection mechanism, the influence of external electric fields on the reaction rate, and the electrical properties of interfaces between diamond and nominally insulating reactant molecules. Here, we report investigations of how an external potential affects the photochemical functionalization reaction, and we compare the effectiveness of the photochemical reaction with that of electrochemical functionalization under similar conditions. We also explore the ability to photochemically pattern the spatial distribution of reactive sites on the surface. Our results provide new insights into the mechanism of the photochemical reaction and how to achieve additional control over the reaction by controlling the electrode potential.

Methods

Sample Preparation. Nanocrystalline diamond films (p-type, B-doped, 0.56 μm thick) were grown on General Electric type 124 fused quartz microscope slides that are transparent at 254 nm. The films were grown at the Naval Research Laboratory

* To whom correspondence may be addressed. E-mail: rjhamers@wisc.edu.
[†] University of Wisconsin−Madison.
[‡] Naval Research Laboratory.

10.1021/jp062443g CCC: $33.50
Published on Web 07/29/2006

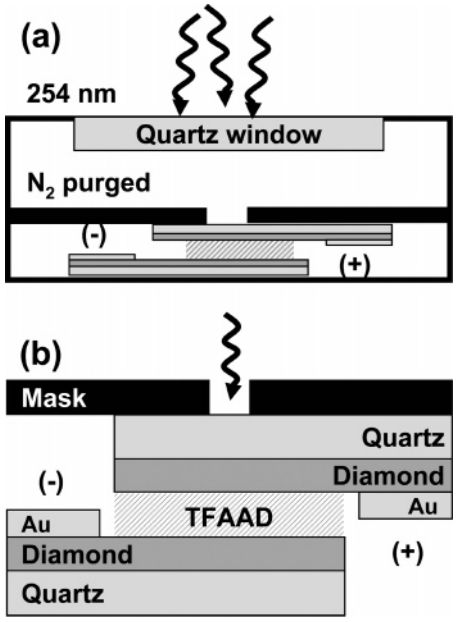

Figure 1. (a) Experimental setup for biased photoelectrochemical reactions. (b) Enlarged view of sample "sandwich" experimental setup (not to scale).

using previously described methods.[21] The samples were cut to dimensions of approximately 1 in. × $^1/_4$ in. and then were masked leaving an approximately $^1/_4$ in. × $^3/_{16}$ in. exposed section; this exposed section was coated with Au using a metal sputter coater (Structure Probe, Inc.). Samples were hydrogen-terminated by exposing to a 13.56 MHz radio frequency hydrogen plasma while heating to ~600 °C for 5 min; the samples were cooled in the plasma for 15 min and then further cooled in pure H_2 for >30 min. Photoelectron spectroscopy measurements show that the resulting surfaces are hydrogen-terminated and are free of oxygen.[17] Following the hydrogen treatment, the sputtered Au layer provides an ohmic contact to the diamond surface.[22]

Sample Functionalization. In previous work[17] we showed that photochemical functionalization of diamond occurs using light at 254 nm. At this wavelength diamond has very low absorbance. We estimate the absorbance of the thin films used here to be <0.1 after correcting for reflection losses. Absorption spectra of the diamond thin films used here, along with other diamond samples investigated previously[17] and shown to functionalize at the same rate, are shown in Supporting Information.

H-terminated nanocrystalline diamond films on fused quartz (H−NCD) were loaded into a nitrogen-purged reaction vessel sealed with a fused quartz window as shown in Figure 1a. The diamond films were separated by a thin fluid layer (~5−10 μL) of TFAAD (trifluoroacetamide-protected 10-aminodec-1-ene) (Figure 1b) that was synthesized and purified as previously described[23] forming a "sandwich"-like structure. Molybdenum clips were used to provide electrical contact to the Au-coated section of the diamond samples for biasing experiments. Biases of up to 5 V were applied; the current flowing between the electrodes (through the fluid film) was simultaneously measured with a picoammeter. Samples were illuminated with 254-nm light from a low-pressure mercury lamp (~1 mW/cm^2) through a $^1/_4$ in. × $^1/_4$ in. window in the Teflon sample holder (Figure 1a,b). The remaining sections of the diamond were shielded from light to prevent photoexcitation at the Au contact and to mitigate any potential side reactions. The photochemical diamond surface reactions were allowed to proceed for a variety of time periods. After the TFAAD-terminated surfaces were removed from the reaction vessel, the samples were sonicated individually in chloroform (5 min) and electronic grade methanol (5 min) to remove any physisorbed material.

Surface Analysis. The photochemically terminated surfaces were analyzed using X-ray photoelectron spectroscopy (XPS) in an ultrahigh vacuum system ($P < 5 \times 10^{-10}$ Torr) equipped with a load-lock for sample introduction, a monochromatized Al Kα source (1486.6 eV), and a hemispherical analyzer with a multichannel detector (resolution = 0.1−0.2 eV). All spectra were collected at 45° photoelectron takeoff angles. Atomic area ratios, denoted as $A_{F(1s)}/A_{C(1s)}$, are used as the principle measure of the extent of functionalization of the diamond surface with TFAAD; these were calculated by fitting the area under the XPS component peaks using Voigt functions with a baseline correction and then correcting for atomic sensitivity factors (C, 0.296; F, 1.00; N, 0.477; O, 0.711).

Electrochemical Analysis. Sheet resistances of the diamond films were measured using a four-point probe. Cyclic voltammetry and impedance spectroscopy measurements were performed in a three-electrode cell using a gold pseudoreference electrode, a gold counter electrode, and hydrogen-terminated diamond as the working electrode. A gold wire was used as a pseudoreference electrode because the Fermi level of gold and of p-type diamond are close in energy;[24] consequently, a potential of 0 V vs the Au reference electrode leads to a situation close to that in the two-electrode cell with 0 V applied between electrodes. All of the electrochemical experiments were performed using vacuum distilled TFAAD that was purged with dry nitrogen prior to measurements. Cyclic voltammograms were measured on a three-electrode potentiostat (Solartron 1287) and impedance analyzer (Solartron 1260) using Corrware (Scribners) software for data acquisition and analysis. To provide higher signal-to-noise, impedance spectra were obtained using a separate current amplifier and dual-phase lock-in amplifier.

Direct Photochemical Patterning and Imaging. To demonstrate the ability to directly photopattern functional groups onto the diamond surface, a H-terminated diamond sample was covered with a thin film of TFAAD, and a molybdenum sheet with 1 mm diameter holes was placed directly on top, forming a simple photomask. This was sealed with a fused quartz window to prevent drying and exposed to 254 nm light for 20 h with no applied bias. The sample was then sonicated in chloroform (10 min) and electronic grade methanol (10 min), dried with nitrogen, and chilled to ~0 °C. The patterned surface was visualized by exposing it to a small amount of water vapor. The resulting pattern was photographed with a Nikon Coolpix digital camera. The sample was again sonicated in electronic grade methanol and then imaged using scanning electron microscopy (SEM, LEO Supra 1555VP) at 2 kV incident electron energy, 11 mm working distance, and imaged with the secondary electron detector biased at +300 V.

Results

Effects of Bias and UV Illumination. To identify the influence of an applied voltage on the reaction process, photochemical reactions were run for varying lengths of time with a 1 V bias applied between the two electrodes using the cell shown in Figure 1. After chemical cleaning steps, XPS was used to measure the C(1s) and F(1s) intensities on a region of each sample that was illuminated and a region that was shielded from direct UV exposure. Figure 2 shows the resulting peak area ratio, $A_{F(1s)}/A_{C(1s)}$ for samples illuminated for the indicated lengths of time. Figure 2a summarizes measurements from

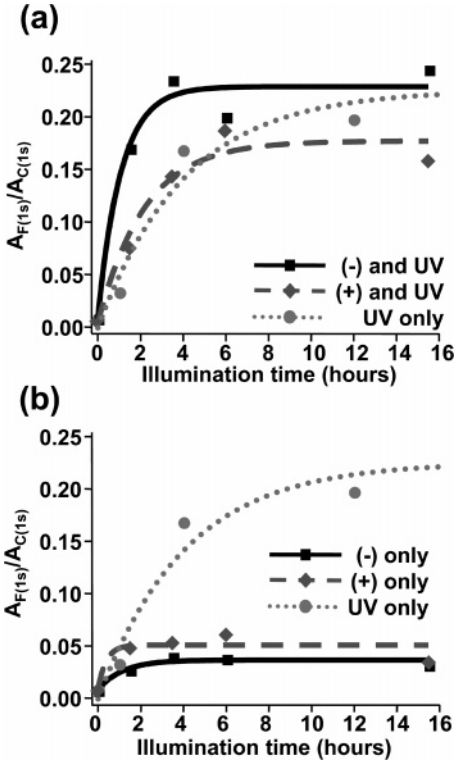

Figure 2. Surface termination of the diamond surface with TFAAD for biased and unbiased samples monitored using XPS: (a) samples exposed to ultraviolet light; (b) samples shielded from ultraviolet light.

regions of the positive and negative electrodes that were exposed to UV light, along with our previously published data for a sample that was exposed to UV light with no applied voltage.[17] Figure 2b shows similar measurements from regions of the same samples that were shielded from the UV light.

In Figure 2a, the data show that the electrode with the negative applied voltage (solid line) is functionalized quickly, yielding $A_{F(1s)}/A_{C(1s)} = 0.17$ after 1.5 h and reaching a terminal value of $A_{F(1s)}/A_{C(1s)} = \sim 0.22$ after only ~3 h of exposure. In contrast, the positively charged electrode (dashed line) yields only $A_{F(1s)}/A_{C(1s)} = 0.07$ after 1.5 h and $A_{F(1s)}/A_{C(1s)} = 0.16$ after ~6 h. The limiting value of $A_{F(1s)}/A_{C(1s)} = 0.22$ for the negatively biased electrode is nearly identical to that measured previously on nanocrystalline and single-crystal diamond samples that were illuminated for >12 h with no applied bias.[17] We thereby conclude that the negative bias enhances the reaction rate on the negative diamond electrode, but the final extent of functionalization (i.e., the monolayer density) is similar to that of the unbiased samples. In contrast, the positively biased electrode is functionalized more slowly than the unbiased sample; while the fluctuations between different samples make it difficult to detect a statistically significant decrease in the initial rate compared with the other samples, the terminal value of $A_{F(1s)}/A_{C(1s)} = 0.16$ observed here after 6 h of illumination of the positive sample is significantly smaller than that observed on the unbiased samples. These data (Figure 2a) show that the rate of functionalization of the diamond surface is accelerated when negatively biased but is much less affected by an equivalent positive bias.

In the biasing experiments immediately above, only part of each sample is exposed to UV light. The remainder of the sample can then act as a "dark" control under biasing conditions identical to the illuminated samples. Figure 2b shows XPS data measured within these dark regions. When a 1 V bias is applied between the samples, the $A_{F(1s)}/A_{C(1s)}$ ratio measured within the dark regions of the negatively (solid line) and positively (dashed line) biased samples are both 0.04−0.05 and are independent of illumination time. For comparison, data for an unbiased photochemical reaction are plotted as a dotted line. The small quantity of fluorinated species on both samples is less than 25% of what is measured on a fully TFAAD-terminated surface and likely arises from a small amount of spontaneous functionalization or trapping of TFAAD at grain boundaries within the polycrystalline film.

The data in Figure 2a were obtained with a 1 V applied potential between the electrodes. To identify how the functionalization rate depended on the magnitude of the applied bias, the composition of the surfaces was analyzed after 1.5 h of UV exposure at biases of 1, 1.5, and 3 V. These surfaces all showed $A_{F(1s)}/A_{C(1s)} = \sim 0.17$ on the UV-exposed sections of the (−) samples and $A_{F(1s)}/A_{C(1s)} \sim 0.06$ on the (+) samples, indicating that there is no significant change in reaction efficiency as the bias is increased from 1 to 3 V. Using an unbiased sample at 1.5 h exposure as a reference point for comparison, we found that in every case the negatively biased samples showed an increased extent of functionalization, while the positively biased samples showed reaction efficiencies similar to the unbiased (but photochemically illuminated) samples.

As an additional control, we conducted experiments in which the positive/negative sample orientation was reversed; those experiments confirmed that the observed differences between positive and negative electrodes were due to the applied bias and not to any differences in optical intensity due to (for example) absorption or scattering within the liquid reactant or top diamond electrode.

Photochemical vs Electrochemical Functionalization. In a previous study of the photochemical functionalization of single-crystal and nanocrystalline diamond, we showed that the reaction was initiated by the ejection of electrons from the H-terminated diamond surface.[17] To test whether a purely electrochemical process might also be able to induce modification of the surface, we compared photochemical and electrochemical functionalization of diamond. To facilitate this comparison, the current between the diamond electrodes was measured during photochemical functionalization experiments. Repeated measurements showed that the measured current during illumination (1.5 V bias) varied significantly from sample to sample, ranging from a few nanoamps to as high as ~130 nA of current. Yet, the XPS data remained very consistent: measurements taken on separate samples exhibiting different currents showed very similar $A_{F(1s)}/A_{C(1s)}$ XPS values. Measurements of the change in current induced by photoexcitation typically showed an increase of approximately 1 nA when the illumination source was turned on. We conclude that in the experiments in which bias is applied, the majority of the current is purely electrochemical and not a direct result of the photoexcitation.

While the current varies from sample to sample, measurements on a single sample set exhibiting a maximum current of 130 nA show that the negatively biased diamond achieved full termination ($A_{F(1s)}/A_{C(1s)} = 0.22$) after a 6 h UV exposure at 1.5 V. From this, we can conclude that in the photoelectrochemical experiment, the surface becomes fully functionalized under conditions where a total of 1.7×10^{16} electrons cross the interface. To test whether full termination could be reached with a similar number of electrons crossing the interface in the absence of UV illumination, H-terminated NCD samples were biased at a potential of 1.5 V in a dark environment while

simultaneously measuring the sample current. The experiments were run until the total number of electrons that flowed through the interface exceeded $\sim 1.7 \times 10^{16}$. In one typical experiment, for example, the sample was biased at 1.5 V for 22 h, during which a minimum of 2.95×10^{17} electrons flowed between the diamond samples, more than an order of magnitude higher than the value observed in photoelectrochemical experiments that achieved full termination. XPS analysis of the negatively biased diamond in this particular experiment showed $A_{F(1s)}/A_{C(1s)} = 0.065$. This value is much smaller than the typical value of 0.22 achieved with only 6 h of UV illumination on a negatively biased sample. We conclude that a purely electrochemical process is not effective at inducing the functionalization. The small amount of F(1s) intensity that is observed is likely due to a combination of some physisorbed material and/or some material that becomes trapped in locations such as grain boundaries in the polycrystalline film.

Photochemical Patterning. One advantage of photochemical functionalization is the potential ability to directly pattern different chemical functional groups onto the surface, using the UV light to control the photochemical reactions. Previous studies have used masks to pattern oxygen and hydrogen on diamond using plasmas[3,25] and lithographic methods to organically pattern diamond surfaces,[11] but direct photochemical patterning of molecular species has not been previously achieved. To pattern the samples, we used physical masks constructed from thin molybdenum sheets that were placed in direct contact with the TFAAD fluid and then covered with a UV-transparent quartz disk to prevent drying, as shown in Figure 3. Simple patterns consisting of holes and lines were investigated. XPS analysis of the photoelectrochemical sample (1 V bias) with a sharp linear boundary, prepared using the setup shown in Figure 1a, shows abrupt transitions in the F(1s) signal and a change in $A_{F(1s)}/A_{C(1s)}$ from 0.05 to 0.22 as the surface is translated over a length of $\sim$1 mm, which is the limiting spatial resolution of our XPS system.

The chemical pattern can easily be observed visually using the fact that the H-terminated diamond is very hydrophobic while the TFAAD molecule is hydrophilic. When samples that have been cooled to near 0 °C are brought into a humid environment, condensation wets the hydrophilic regions but forms very small water drops on the hydrophobic regions. Consequently, the hydrophobic regions have increased diffuse scattering of light, while the hydrophilic regions do not. Depending on whether the sample is observed in off-specular or near-specular directions with respect to a light source, the TFAAD-modified regions can appear lighter or darker than the surrounding H-terminated regions. Figure 3b shows a visible-light image of a sample that was patterned using a simple molybdenum mask with 1 mm diameter holes where the TFAAD-modified section of the surface appears darker than the H-terminated section.

The chemical patterning of the surface can also be viewed at higher resolution directly using scanning electron microscopy due to the differences in secondary electron yield. Figure 3c shows an SEM image of a 1 mm diameter TFAAD-functionalized region surrounded by H-terminated diamond. Analysis of the SEM images in cross section shows that the transition from TFAAD-functionalized to H-terminated regions is very sharp, with a width of $<25\ \mu$m (Figure 3d). The ability to retain a sharp boundary has an important mechanistic implication by demonstrating that diffusion of reactive species in the liquid phase over time periods of many hours does not alter the spatial distribution of functionalized sites on the surface.

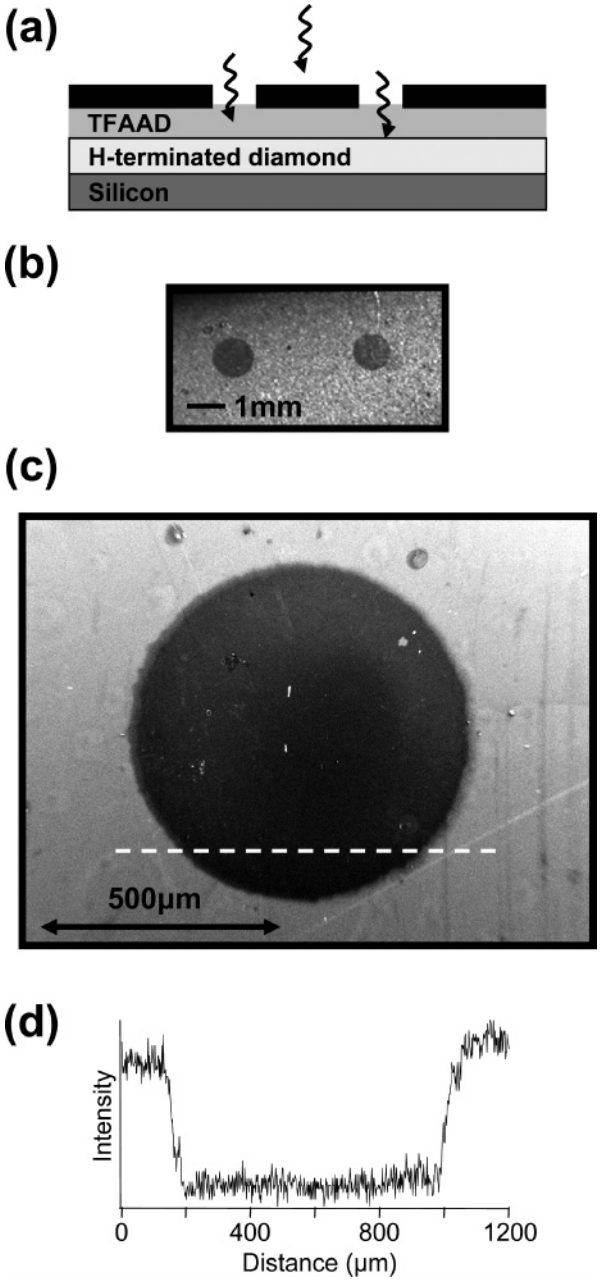

Figure 3. (a) Experimental setup for photochemical 1 mm mask patterning. (b) Digital photograph of H-terminated diamond (light areas) photochemically patterned with TFAAD (dark spots) visualized by hydrophobic/hydrophilic interactions with water vapor. (c) SEM image of photopatterned 1 mm TFAAD spot on hydrogen-terminated diamond. (d) Contrast profile corresponding to dashed line in (c).

Electrical Properties of the Diamond−TFAAD Interface. When a four-point probe was used, the sheet resistance of the diamond films was determined to be $1.3 \times 10^5\ \Omega$/square; using the known thickness of the diamond film (0.56 μm), this yields a conductivity of 7.2 Ω cm. Measurements made with the UV light on and light off show differences in the total sheet current and the measured voltage, but the overall sheet resistance does not change; this indicates that the number of mobile charge carriers produced by illumination is small compared with those produced by the bulk doping. Knowing this bulk conductivity is important because it establishes that during all photochemical and electrochemical functionalization experiments, the resistance along the length of the diamond film (i.e., between the external contacts and the illuminated region) is sufficiently small that the voltage drop along the film is <10 mV, even at the highest

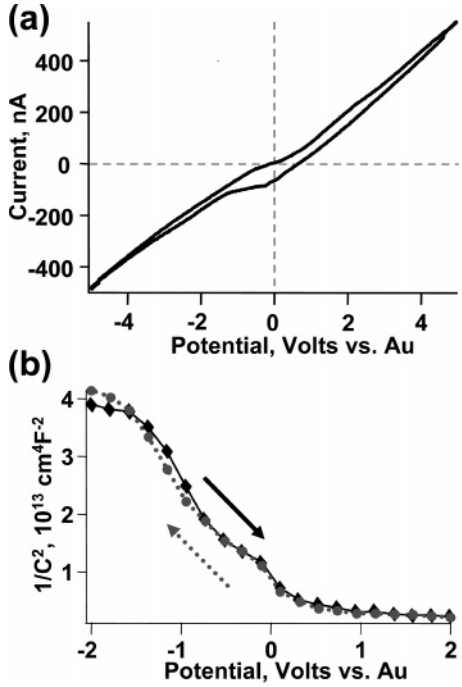

Figure 4. Electrochemical data for diamond vs Au pseudoreference electrode in neat TFAAD: (a) cyclic voltammogram (50 mV/s) demonstrating capacitive behavior between −1 and +0.2 V; (b) Mott−Schottky plot showing sigmoidal shape characteristic of doped semiconductors.

currents observed. We also note that gold is known to make an ohmic contact to H-terminated diamond,[22] which we have verified independently. These measurements establish that when a bias is applied to the gold contacts sputtered onto the diamond electrodes, the potential is dropped in the space-charge region of the diamond or within the TFAAD, rather than along the length of the diamond electrodes or at the contacts.

To identify whether it is the semiconductor space-charge layer or the liquid film that ultimately limits the conductivity of the system, electrochemical measurements of the diamond−TFAAD interface were made. To avoid contamination or undesired introduction of ionic materials into the TFAAD, a thin-layer cell incorporating a simple pseudoreference electrode consisting of a clean gold wire was used. The work function of polycrystalline gold is approximately 4.7−4.8 eV.[24] Assuming an electron affinity of −0.5 V[17] and a Fermi energy lying ∼0.3−0.7 V above the valence band maximum,[26,27] the vacuum level of diamond lies 4.3−4.7 eV above its Fermi level. Accordingly, we expect a contact potential difference of no more than a few tenths of a volt between the gold pseudoreference electrode and the diamond samples, such that the potential of 0 V vs this pseudoreference electrode is reasonably close to the open-circuit condition for the two-electrode cell.

Figure 4a shows a cyclic voltammogram of the cell, where the potentials are all referenced to the gold pseudoreference electrode. At voltages of <-2 V and $>+2$ V with a scan rate of 50 mV/s, the cell exhibits a clear linear dependence of current on voltage, indicating simple ohmic behavior. At voltages between approximately −1 and +0.2 V, however, the separation between forward and reverse sweeps increases, leading to a region exhibiting a more rectangular shape; this is characteristic of a capacitive response, in which the current flow, $I = C^* \mathrm{d}V/\mathrm{d}t$, is significantly different on the forward and backward sweeps due to the different sign of $\mathrm{d}V/\mathrm{d}t$. The rectangular shape indicates that within this potential range, the response of the system is dominated by capacitance.

Electrochemical impedance spectroscopy measurements were used to identify whether this capacitance arises from the diamond space-charge region or from an electrochemical double-layer in the fluid. In these measurements, the real (Z') and imaginary (Z'') components of the complex impedance Z, where $Z = Z' + iZ''$, are extracted by applying a sinusoidal modulation to the applied potential and measuring the in-phase and out-of-phase components of the current flowing across the interface. Such measurements are typically made as a function of frequency and potential. In a simple resistance−capacitance model of the interface, the capacitance is directly related to the imaginary part (Z'') of the complex impedance as

$$C = \frac{-1}{2\pi f Z''}$$

Our measurements of capacitance as a function of potential show a distinct sigmoidal shape, with a higher capacitance at more positive potentials and lower capacitance at potentials more negative than ∼ −1 V. This shape is significant: the capacitance−voltage characteristics of doped semiconductors are sigmoidal, while the capacitance−voltage characteristics of dilute ionic liquids are approximately parabolic in shape.[28] For semiconductors, the capacitance−voltage characteristics are usually plotted as a "Mott−Schottky" plot of $1/C^2$ vs potential. Figure 4b shows a Mott−Schottky plot of capacitance data that were measured at 103 Hz. The pronounced sigmoidal shape is readily apparent and is similar to that anticipated for a p-type semiconductor. When biased at positive potentials, a typical p-type semiconductor is expected to have upward band-banding, forcing the semiconductor into the accumulation region in which there is a very high density of charges near the surface; this leads to a high capacitance and a low $1/C^2$. At negative potentials, a p-type semiconductor would be expected to have downward band-banding; this leads to a depletion of charge carriers, yielding a small capacitance and a large $1/C^2$. In our system, the interpretation is complicated by the fact that there is a parallel conductive pathway that turns on at potentials more negative than −1 V and more positive than ∼+0.2 V and because there may be some contribution from the electrochemical double-layer in the fluid. Yet, the data clearly show an asymmetry in C vs V that is like that expected for a semiconductor−electrolyte interface in which the applied potential induces a band-bending in the semiconductor. In contrast, the electrical double layers formed by ions in solution (or, what might be anticipated from any ions present in the reactant fluid) vary quadratically with voltage.[28] The capacitance−voltage data establish that as the sample potential is varied between −1.0 and + 0.2 V, the resulting electric field significantly changes the band-bending within the diamond space-charge region.

Discussion

The photochemical functionalization of H-terminated diamond is an extremely interesting reaction because in addition to giving rise to interfaces exhibiting extraordinarily high chemical stability, the mechanism itself is unusual, occurring with sub-band-gap light. Previous studies on H-terminated surfaces of silicon[29,30] and diamond[31] have shown that radicals in solution can abstract H atoms from the H-terminated surfaces, leaving behind highly reactive surface "dangling bonds" that can then link to reactant molecules in solution. Once a dangling bond is created, reaction with alkenes in solution is expected to be facile.[23,32−36] On the basis of these studies, we expect that the functionalization of diamond with organic alkenes can be divided into two discrete steps: (1) initiation by the creation of

a surface dangling bond and (2) the subsequent reaction of the dangling bond with the alkenes. The second step is well understood based on previous work.[29−31] However, the photochemical initiation step remains poorly understood, even on well-studied surfaces such as silicon.

Our previous study showed that the ability to functionalize H-terminated surfaces of single-crystal and nanocrystalline diamond using 254 nm light (photon energy = 4.88 eV) was closely connected to the ability to eject photoelectrons into the adjacent reactive fluid.[17] This process is facilitated by the negative electron affinity (NEA) of the surface. NEA implies that the vacuum level is lower in energy that the conduction band, such that conduction-band electrons can be easily ejected out of the diamond. We proposed that the ejection of these electrons into the adjacent fluid ("internal photoemission") can lead to creation of radicals and other reactive species in the fluid that in turn could abstract a hydrogen atom from the H-terminated diamond, leaving "dangling bonds" on the surface. The highly reactive dangling bonds allow for subsequent propagation steps of the proposed radical-based mechanism. We inferred the existence of these radicals by direct observation of changes in the chemical composition of the liquid phase upon exposure to H-diamond surfaces illuminated with 254 nm light.

As part of the question of how the functionalization of diamond is initiated with sub-band-gap light, the possible role of electric fields within the semiconductor space-charge region and/or in the organic fluid phase, and whether functionalization can be initiated electrochemically without UV light become very important. Understanding the photochemical mechanism is also significant for understanding the ultimate spatial resolution that might be achievable using UV light to photopattern chemical functional groups onto specific locations of the sample.

We first address the influence of an externally applied potential. Our data in Figure 2 clearly show that applying a 1 V potential across a sandwich of diamond electrodes separated by TFAAD enhances the reaction rate at the negative electrode by approximately a factor of 3 and slightly decreases the rate at the positive electrode. The influence of the applied bias on the reaction rate could be associated with the presence of an electric field in the semiconductor (i.e., field-induced band-bending) or by an electric field in the fluid that might (for example) attract or repel charged species from the electrodes. In both cases, higher potentials would be expected to further influence the reaction rate. Yet, our XPS measurements show that while there is a clear enhancement in functionalization rate for applied voltages of ~1 V, higher voltage (up to ~3 V, the maximum tested) does not further increase the rate. To fully understand the lack of change in functionalization rate between 1 and 3 V requires understanding how the electric field is distributed between the fluid and the semiconductor surface.

The electrochemical data in Figure 4 provide insight into the potential drops. The existence of a ohmic region at potentials more negative than approximately −1 V or more positive than approximately 0.2 V (vs a Au pseudoreference electrode) implies that in this region the applied potential is driving an electrochemical reaction (a Faradaic process). *Within* the narrow potential window between −1.0 and +0.2 V, however, the nearly rectangular shape of the $I-V$ curve shows that under these conditions the overall cell impedance is limited by capacitance. This capacitive behavior could in principle be associated with either the diamond space-charge layer, the bulk fluid, or an electrical double-layer that could exist in the fluid at the semiconductor−TFAAD interface if ionic species were present in the TFAAD. The sigmoidal shape of the Mott−Schottky plot in Figure 4b mirrors the expected behavior for a p-type semiconductor. At negative potentials the surface bands are bent downward, forming a depletion region that has only a small space-charge capacitance. Conversely, at the positive electrode the applied field would be expected to induce an upward band-bending; however, for a p-type sample it is difficult to induce upward band-bending, especially as the Fermi level comes close to the boron acceptor level that lies 0.37 eV above the valence band.[37] The data in Figure 4b strongly suggest that the application of an electric field across the diamond−fluid interface induces a significant band-bending within the negatively biased diamond sample, which is responsible for the influence of applied bias on the functionalization rate.

This observation is significant because previous studies of photoemission from diamond using sub-band-gap illumination have identified two possible mechanisms. One mechanism involves photoexcitation of electrons from mid-gap (defect- or dopant-related) electronic states to the conduction band, followed by drift to the surface and then ejection of the electrons into vacuum.[38−42] A second mechanism involves electron ejection directly from the valence band into vacuum.[43] Previous studies have suggested the mechanism involving excitation to the conduction band via mid-gap defect states is more favorable because it takes advantage of a longer optical absorption depth and has less stringent momentum conservation rules.[44] Since the electric field clearly has a large influence on the functionalization rate, our data support the defect-mediated excitation to the conduction band followed by electron ejection.

Figure 5 depicts how the applied potential influences the bands in the context of the "sandwich" structure. Previous studies have shown that H-terminated samples of B-doped diamond typically have downward band-bending and exhibit negative electron affinity.[17,42,45,46] Several researchers have reported that undoped samples that were H-terminated and then exposed to air or water can transfer electrons to the water thin films, resulting in an upward band-bending and formation of a conductive p-type surface region.[47,48] In a previous study,[17] we showed that boron-doped samples that were hydrogen-terminated and then immediately transferred to vacuum or immediately functionalized with organic layers both retain the downward banding that is characteristic of the freshly H-terminated sample. This downward band-bending induced by the H-termination is one of the key factors controlling the negative electron affinity of H-terminated diamond. For two diamond samples in electrical contact at zero applied bias, the Fermi levels of both samples are aligned and the bands are bent slightly downward, as in Figure 5a.[49] As the potential is increased (Figure 5b), the negatively biased electrode has its bands bent downward, and we observe an increased functionalization rate. Conversely, the positively biased sample may have its bands bent slightly upward with little change in the initial functionalization rate. Our data therefore suggest that the bias-dependent changes in functionalization are a direct result of the band-bending induced in the diamond space-charge layers, which in turn influences the rate of electron ejection when illuminated with 254 nm light.

Our data suggest that photoexcitation events excite electrons from mid-gap bulk defect states to the conduction band as depicted in Figure 5c. Drift in the space-charge layer can drive the electrons toward the surface, from where they can be easily ejected. The drift and photoemission can occur at zero bias because of the intrinsic downward band-bending,[49] but these processes can be enhanced or hindered by the application of an additional electric field. In a previous study we showed that

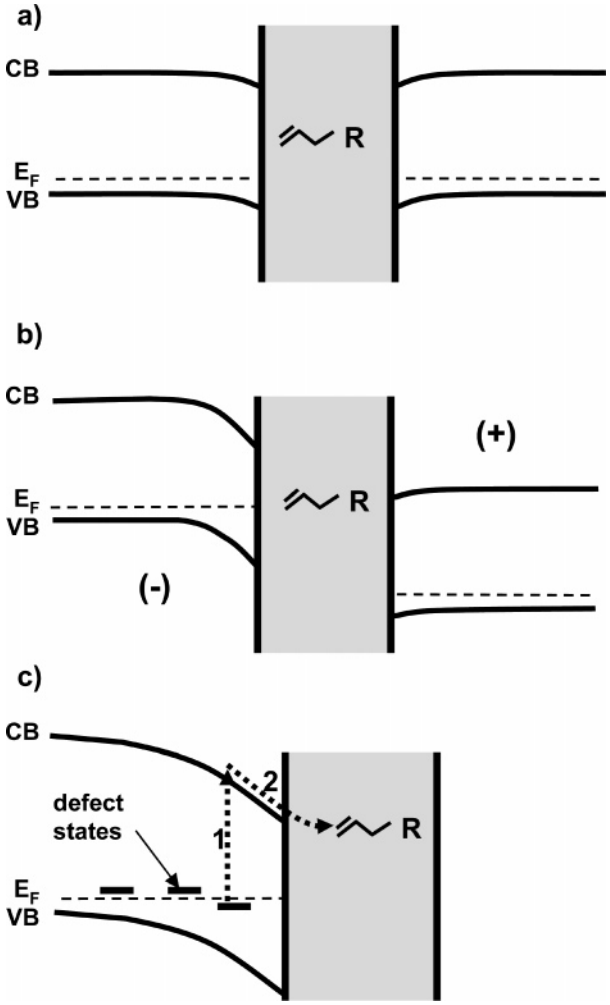

Figure 5. Band diagram for "sandwich" sample orientation with (a) no applied bias, (b) applied bias, and (c) photochemical ejection.

the electron ejection creates reaction products that can be directly detected by analysis of the liquid.[17] As depicted in Figure 6, we hypothesize that the emission of electrons creates radical anions (Figure 6a) that most likely operate by abstracting a H atom from the H-terminated diamond surface, creating an unsaturated carbon "dangling bond" at the surface (Figure 6b,c). We note that alkenyl anions have very diffuse electronic structures,[50,51] such that the Lewis dot structures in Figure 6 do not necessarily reflect the precise locations of the charges and unpaired electrons. Once such a surface radical species is formed, its reactions are likely similar to those for photochemical functionalization of silicon, involving reactions of surface radicals with additional alkene molecules (neutral or radical) in the liquid phase, as depicted in Figure 6d.

At higher voltages, our data demonstrate the turn-on of a Faradaic process. While the nature of this reaction is not known, the ~1.2 V window where there are no Faradaic reactions is very similar to that expected for water at pH ~7. Our TFAAD has been vacuum distilled and is not expected to contain any significant amount of water, but it is nearly impossible to rule out trace amounts of water or other contaminants that might give rise to the 10^7 Ω resistance that we observe experimentally at large bias. The linear $I-V$ curve in Figure 4a indicates that at these higher voltages the current is limited by a resistive element, which we attribute to the resistance of the fluid (TFAAD with possibly trace impurities such as water). The data indicate that as the applied voltage is increased above approximately 1 V and Faradaic processes become significant,

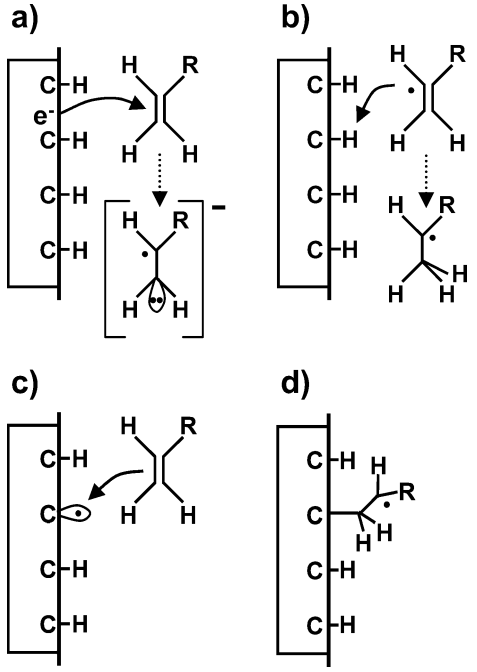

Figure 6. Proposed mechanism for monolayer formation: (a) electron ejection and solution radical formation; (b) hydrogen abstraction from the diamond surface; (c) interaction of surface dangling bond with neutral alkene in solution; (d) resulting surface-bound radical species. Subsequent reactions are not shown.

TABLE 1: Comparison of Current between Diamond Samples during Dark and Illuminated Experiments

	UV	dark
time (h)	6	22
potential (V)	1.5	1.5
no. of electrons	1.75×10^{16}	2.59×10^{17}
$A_{F(1s)}/A_{C(1s)}$	0.22	0.065

most of the additional potential drop occurs across the fluid rather than across the diamond space-charge layer. These higher potentials do not lead to additional band-bending and do not affect the photochemical reaction rate. Moreover, these purely electrochemical reactions do not lead to functionalization of the surface.

Photoelectrochemical vs Electrochemical Functionalization. When a steady bias is applied between diamond electrodes, there are two types of current that flow. In the absence of UV illumination, there is a significant electrochemical background current that gives rise to the ohmic behavior in Figure 4a. In the presence of UV illumination, there is an additional photocurrent or, more properly, a photoelectrochemical current. In experiments where we have directly measured the current between the positively and negatively biased diamond electrodes, the difference in current between "dark" and "illuminated" samples is typically very small, on the order of 1 nA, while the purely electrochemical background current can be much larger, 100 nA or more. Yet, Table 1 shows that the purely electrochemical integrated current is not effective in promoting the surface functionalization *even though it is approximately 10 times larger than the UV-induced photoelectrochemical current*. This implies that the charge carriers responsible for the photochemical functionalization are in different electronic states than those that induce the background electrochemical current. Since the band gap of diamond is 5.5 eV, the Faradaic current that occurs with potentials as small as ~1 V must involve mid-gap states. In contrast, the electrons responsible for initiating the photochemical functionalization

are likely in higher energy states, such as the diamond conduction band. While the precise details of the states involved in functionalization of diamond remain uncertain, it is clear that the charge carriers involved in photochemical functionalization of diamond are distinct from those that participate in purely electrochemical reactions under moderate conditions.

Photochemical Patterning. Figure 3 shows that it is possible to directly photopattern the spatial distribution of chemical groups on the surface. We achieved a spatial resolution of ~25 μm using a simple contact mask. Since the fluid layer itself is likely ~25 μm in thickness, the resolution is most likely limited by the mask-to-substrate distance. The ability to pattern on this length scale is important mechanistically because in our proposed mechanism electron ejection creates reactive molecules (such as radical anions) in the liquid phase. Our results suggest that any diffusion of reactive molecules in the liquid phase is small enough that it does not degrade resolution on a 25 μm scale.

Summary of Reaction Pathway. The overall photochemical surface termination can be divided into two stages: (1) the creation of a surface dangling bond and (2) the subsequent reaction of the dangling bond with olefinic groups of the adjacent liquid. The reaction of surface dangling bonds with liquid-phase alkenes has been widely established in a number of studies of silicon[29,32−35,52,53] and is not expected to be significantly different on H-terminated diamond. While surface radicals on both silicon[29,54] and diamond[31] can be created by intentional addition of radical initiators such as diacyl peroxide or benzoyl peroxide to the liquid phase, the mechanism by which reactions are initiated photochemically is more complex. Even on silicon, it remains controversial whether the reaction is initiated by photochemical cleavage of Si−H bonds or through an electron−hole pair mechanism.[32,33,35,53] In the case of diamond, we showed previously that there is no direct C−H bond cleavage at the hydrogen-terminated diamond surface[17] and instead that the photochemical functionalization is associated with direct electron ejection, forming radical anions in solution.[17] The abstraction of a hydrogen atom from the H-terminated diamond surface would then lead to functionalization in a straightforward manner analogous to the reactions on silicon. For unbiased electrodes, the ejection of electrons must eventually be balanced by an oxidation reaction at the surface. The nature of this reaction remains unknown, but one possibility would be the oxidation of water. In this respect, there is also a strong complementarity to the well-known photocatalytic reactions of TiO_2, in which photoexcited holes induce surface oxidation reactions of organic species and the electrons are involved in reduction of water or oxygen.[55] With diamond, the very high energy of the conduction band facilitates electron ejection that must be balanced by some type of oxidation reaction.

The photochemical termination of diamond is interesting because it can also be applied to a number of other materials that are otherwise difficult to functionalize. For example, the same procedure can be used to functionalize carbon nanofibers[56] and glassy carbon.[19] The graphitic structures of these materials give them lower work functions than diamond, with typical values of ~4.6 eV for carbon nanofibers[57] and 4.7 eV for graphite.[58] These values are slightly smaller than the 4.88 eV energy of a 254 nm photon, so that ejection of photoelectrons is very likely when illuminated with 254 nm light. It is likely that the photochemical functionalization can be applied to other semiconductor materials as well.

Conclusions

Our studies show that the functionalization of H-terminated diamond with organic alkenes occurs by a unique mechanism in which reactive species are created immediately adjacent to the surface via photoemission of electrons from the diamond into the fluid. Our bias-dependent studies show how electric fields can influence the reaction by controlling the diffusion of photoexcited electrons in the conduction band. This underscores the importance of the high-energy conduction-band electrons in facilitating the reaction, as only these electrons have sufficient energy to be ejected into the fluid and create radical species at the solid−liquid interface. These reactive liquid-phase species facilitate the reaction by abstracting H atoms from the surface C−H species, thereby allowing the surface to undergo radical reactions with organic alkenes. To the best of our knowledge, the photoemission of electrons has not been used previously to create well-defined monolayer films on surfaces of semiconductors or other materials. The use of photochemical methods to directly pattern the spatial distribution of chemical functional groups provides a pathway for fabrication of more complex surfaces that take advantage of the very high stability of diamond and the ability to control its chemical, biochemical, and physical properties by controlling the chemistry of the surface.

Acknowledgment. This work is supported by the National Science Foundation Grant CHE-0314618 and DMR-0210806. J.E.B. and J.N.R. were funded in part by the Office of Naval Research/Naval Research Laboratory. The assistance of Tatyana Feygelson in preparing the nanocrystalline diamond films is greatly appreciated.

Supporting Information Available: Ultraviolet absorption spectra of the diamond-on-quartz samples used in this study, along with comparison of a single-crystal type IIb natural diamond. This material is available free of charge via the Internet at http://pubs.acs.org

References and Notes

(1) May, P. W. *Philos. Trans. R. Soc., London A* **2000**, *358*, 473.
(2) Wei, J.; Yates, J. T., Jr. *Crit. Rev. Surf. Chem.* **1995**, *5*, 1.
(3) Hartl, A.; Schmich, E.; Garrido, J. A.; Hernando, J.; Catharino, S. C. R.; Walter, S.; Feulner, P.; Kromka, A.; Steinmuller, D.; Stutzmann, M. *Nat. Mater.* **2004**, *3*, 736.
(4) Garrido, J. A.; Hartl, A.; Kuch, S.; Stutzmann, M.; Williams, O. A.; Jackmann, R. B. *Appl. Phys. Lett.* **2005**, *86*.
(5) Yang, W. S.; Hamers, R. J. *Appl. Phys. Lett.* **2004**, *85*, 3626.
(6) Yang, W. S.; Butler, J. E.; Russell, J. N., Jr.; Hamers, R. J. *Langmuir* **2004**, *20*, 6778.
(7) Kuo, T. C.; McCreery, R. L.; Swain, G. M. *Electrochem. Solid-State. Lett.* **1999**, *2*, 288.
(8) Liu, Y.; Gu, Z. N.; Margrave, J. L.; Khabashesku, V. N. *Chem. Mater.* **2004**, *16*, 3924.
(9) Ohta, R.; Saito, N.; Inoue, Y.; Sugimura, H.; Takai, O. *J. Vac. Sci. Technol., A* **2004**, *22*, 2005.
(10) Wenmackers, S.; Christiaens, P.; Deferme, W.; Daenen, M.; Haenen, K.; Nesladek, M.; Wagner, P.; Vermeeren, V.; Michiels, L.; van de Ven, M.; Ameloot, M.; Wouters, J.; Naelaerts, L.; Mekhalif, Z. Functionally Graded Materials VIII, 2005; Vol. 492−493.
(11) Zhang, G. J.; Umezawa, H.; Hata, H.; Zako, T.; Funatsu, T.; Ohdomari, L.; Kawarada, H. *Jpn. J. Appl. Phys., Part 2* **2005**, *44*, L295.
(12) Tsubota, T.; Ida, S.; Hirabayashi, O.; Nagaoka, S.; Nagata, M.; Matsumoto, Y. *Phys. Chem. Chem. Phys.* **2002**, *4*, 3881.
(13) Ida, S.; Tsubota, T.; Hirabayashi, O.; Nagata, M.; Matsumoto, Y.; Fujishima, A. *Diamond Relat. Mater.* **2003**, *12*, 601.
(14) Kim, C. S.; Mowrey, R. C.; Butler, J. E.; Russell, J. N., Jr. *J. Phys. Chem. B* **1998**, *102*, 9290.
(15) Miller, J. B. *Surf. Sci.* **1999**, *439*, 21.
(16) Strother, T.; Knickerbocker, T.; Russell, J. N., Jr.; Butler, J. E.; Smith, L. M.; Hamers, R. J. *Langmuir* **2002**, *18*, 968.
(17) Nichols, B. M.; Butler, J. E.; Russell, J. N., Jr.; Hamers, R. J. *J. Phys. Chem. B* **2005**, *109*, 20938.

(18) Yang, W. S.; Auciello, O.; Butler, J. E.; Cai, W.; Carlisle, J. A.; Gerbi, J. E.; Gruen, D. M.; Knickerbocker, T.; Lasseter, T.; Russell, J. N., Jr.; Smith, L. M.; Hamers, R. J. *Nat. Mater.* **2002**, *1*, 253.
(19) Lasseter, T. L.; Clare, B. H.; Abbott, N. L.; Hamers, R. J. *J. Am. Chem. Soc.* **2004**, *126*, 10220−10221.
(20) Clare, T. L.; Clare, B. H.; Nichols, B. M.; Abbott, N. L.; Hamers, R. J. *Langmuir* **2005**, *21*, 6344.
(21) Butler, J. E.; Windischmann, H. *Mater. Res. Bull.* **1998**, *23*, 22.
(22) Mori, Y.; Kawarada, H.; Hiraki, A. *Appl. Phys. Lett.* **1991**, *58*, 940.
(23) Strother, T.; Hamers, R. J.; Smith, L. M. *Nucleic Acids Res.* **2000**, *28*, 3535.
(24) Trasatti, S. *Electroanal. Chem.* **1974**, *54*, 19.
(25) Park, M.; Choi, W. B.; Streiffer, S. K.; Hren, J. J.; Cuomo, J. J. *Appl. Phys. Lett.* **1998**, *72*, 2580.
(26) Cui, J. B.; Ristein, J.; Ley, L. *Phys. Rev. Lett.* **1998**, *81*, 429.
(27) Diederich, L.; Aebi, P.; Kuttel, O. M.; Schlapbach, L. *Surf. Sci.* **1999**, *424*, L314.
(28) Bard, A. J.; Faulkner, L. R. *Electrochemical methods: fundamentals and applications*, 2nd ed.; Wiley: New York, 2001.
(29) Linford, M. R.; Fenter, P.; Eisenberger, P. M.; Chidsey, C. E. D. *J. Am. Chem. Soc.* **1995**, *117*, 3145.
(30) Niederhauser, T. L.; Jiang, G.; Lua, Y.-Y.; Dorff, M.; Woolley, A. T.; Asplund, M. C.; Berges, D. A.; Linford, M. R. *Langmuir* **2001**, *17*, 5889.
(31) Tsubota, T.; Hirabayashi, O.; Ida, S.; Nagoka, S.; Nagata, M.; Matsumoto, Y. *Diamond Relat. Mater.* **2002**, *11*, 1360.
(32) Stewart, M. P.; Buriak, J. M. *J. Am. Chem. Soc.* **2001**, *123*, 7821.
(33) Stewart, M. P.; Buriak, J. M. *Angew. Chem., Int. Ed. Engl.* **1998**, *37*, 3257.
(34) Cicero, R. L.; Chidsey, C. E. D.; Lopinski, G. P.; Wayner, D. D. M.; Wolkow, R. A. *Langmuir* **2002**, *18*, 305.
(35) Cicero, R. L.; Linford, M. R.; Chidsey, C. E. D. *Langmuir* **2000**, *16*, 5688.
(36) Strother, T.; Cai, W.; Zhao, X. S.; Hamers, R. J.; Smith, L. M. *J. Am. Chem. Soc.* **2000**, *122*, 1205.
(37) Glesener, J. W. *Appl. Phys. Lett.* **1994**, *64*, 217.
(38) Ristein, J.; Stein, W.; Ley, L. *Phys. Rev. Lett.* **1997**, *78*, 1803.
(39) Vouagner, D.; Show, Y.; Kiraly, B.; Champagnon, B.; Girardeau-Montaut, J. P. *Appl. Surf. Sci.* **2000**, *168*, 79.
(40) Cui, J. B.; Ristein, J.; Ley, L. *Phys. Rev. B* **1999**, *60*, 16135.
(41) Cui, J. B.; Stammler, M.; Ristein, J.; Ley, L. *J. Appl. Phys.* **2000**, *88*, 3667.
(42) Ristein, J.; Stein, W.; Ley, L. *Diamond Relat. Mater.* **1998**, *7*, 626.
(43) Takeuchi, D.; Kato, H.; Ri, G. X.; Yamada, T.; Vinod, P. R.; Hwang, D.; Nebel, C. E.; Okushi, H.; Yamasaki, S. *Appl. Phys. Lett.* **2005**, *86*, 152103.
(44) Bandis, C.; Pate, B. B. *Phys. Rev. Lett.* **1995**, *74*, 777.
(45) Diederich, L.; Kuttel, O.; Aebi, P.; Schlapbach, L. *Surf. Sci.* **1998**, *418*, 219.
(46) Bandis, C.; Pate, B. B. *Phys. Rev. B* **1995**, *52*, 12056.
(47) Maier, F.; Riedel, M.; Mantel, B.; Ristein, J.; Ley, L. *Phys. Rev. Lett.* **2000**, *85*, 3472.
(48) Ristein, J.; Cui, J. B.; Graupner, R.; Maier, F.; Riedel, M.; Mantel, B.; Stammler, M.; Ley, L. *New Diamond Front. Carbon Technol.* **2000**, *10*, 363.
(49) Williams, O. A.; Whitfield, M. D.; Jackman, R. B.; Foord, J. S.; Butler, J. E.; Nebel, C. E. *Appl. Phys. Lett.* **2001**, *78*, 3460.
(50) Itoh, K.; Holroyd, R. A.; Nishikawa, M. *J. Phys. Chem. B* **1998**, *102*, 3147.
(51) Staley, S. W.; Howard, A. E.; Strnad, J. T. *J. Org. Chem.* **1992**, *57*, 895.
(52) Linford, M. R.; Chidsey, C. E. D. *Langmuir* **2002**, *18*, 6217.
(53) Langner, A.; Panarello, A.; Rivillon, S.; Vassylyev, O.; Khinast, J. G.; Chabal, Y. J. *J. Am. Chem. Soc.* **2005**, *127*, 12798.
(54) Buriak, J. M. *Chem. Rev.* **2002**, *102*, 1271.
(55) Lu, G.; Linsebigler, A.; Yates, J. T., Jr. *J. Phys. Chem.* **1995**, *99*, 7626.
(56) Baker, S. E.; Tse, K. Y.; Hindin, E.; Nichols, B. M.; Clare, T. L.; Hamers, R. J. *Chem. Mater.* **2005**, *17*, 4971.
(57) Nichols, B. M. Unpublished data, 2005.
(58) Hansen, W. N.; Hansen, G. J. *Surf. Sci.* **2001**, *481*, 172.